salts-catalyzed aza-Michael reactions of enones with carbamates. Org Lett **18**: 1319-22.

25. **Koutsoudakis, G., E. Herrmann, S. Kallis, R. Bartenschlager, and T. Pietschmann.** 2007. The level of CD81 cell surface expression is a key determinant for productive entry of hepatitis C virus into host cells. J Virol **81:**588-98.

26. **Lohmann, V., F. Korner, J. Koch, U. Herian, L. Theilmann, and R. Bartenschlager.** 1999. Replication of subgenomic hepatitis C virus RNAs in a hepatoma cell line. Science **285:**110-3.

27. **Mackenzie, J. M., and E. G. Westaway.** 2001. Assembly and maturation of the flavivirus Kunjin virus appear to occur in the rough endoplasmic reticulum and along the secretory pathway, respectively. J Virol **75:**10787-99.

28. **Manes, S., G. del Real, R. A. Lacalle, P. Lucas, C. Gomez-Mouton, S. Sanchez-Palomino, R. Delgado, J. Alcami, E. Mira, and A. C. Martinez.** 2000. Membrane raft microdomains mediate lateral assemblies required for HIV-1 infection. EMBO **1**: 190-6.

29. Matsuo, E., H. Tani, C. Lim, Y. Komoda, T. Okamoto, H. Miyamoto, K. Moriishi, S. Yagi, A.H. Patel, T. Miyamura, and Y. Matsuura. 2006. Characterization of HCV-like particles produced in a human hepatoma cell line by a recombinant baculovirus. Biochem Biophys Res Commun. **340**:200-8.

30. **Matto, M., C. M. Rice, B. Aroeti, and J. S. Glenn.** 2004. Hepatitis C virus core protein associates with detergent-resistant membranes distinct from classical plasma membrane rafts. J Virol **78:**12047-53.

31. **Miyake, Y., Y. Kozutsumi, S. Nakamura, T. Fujita, and T. Kawasaki.** 1995. Serine palmitoyltransferase is the primary target of a sphingosine-like immunosuppressant, ISP-1/myriocin. Biochem Biophys Res Commun **211:**396-403.

32. **Miyanari, Y., K. Atsuzawa, N. Usuda, K. Watashi, T. Hishiki, M. Zayas, R. Bartenschlager, T. Wakita, M. Hijikata, and K. Shimotohno,** 2007. The lipid droplet is an important organelle for hepatitis C virus production. Nat Cell Biol **9**: 1089-97.

33. **Morikawa, K., Z. Zhao, T. Date, M. Miyamoto, A. Murayama, D. Akazawa, J. Tanabe, S. Sone, and T. Wakita.** 2007. The roles of CD81 and glycosaminoglycans in the adsorption and uptake of infectious HCV particles. J Med Virol **79:**714-23.

34. **Murakami, K., K. Ishii, Y. Ishihara, S. Yoshizaki, K. Tanaka, Y. Gotoh, H. Aizaki, M. Kohara, H. Yoshioka, Y. Mori, N. Manabe, I. Shoji, T. Sata, R. Bartenschlager, Y. Matsuura, T. Miyamura, and T. Suzuki.** 2006. Production of infectious hepatitis C virus particles in three-dimensional cultures of the cell line carrying the genome-length dicistronic viral RNA of genotype 1b. Virology

351:381-92.

35. **Nakai, K., T. Okamoto, T. Kimura-Someya, K. Ishii, C. K. Lim, H. Tani, E. Matsuo, T. Abe, Y. Mori, T. Suzuki, T. Miyamura, J. H. Nunberg, K. Moriishi, and Y. Matsuura.** 2006. Oligomerization of hepatitis C virus core protein is crucial for interaction with the cytoplasmic domain of E1 envelope protein. J Virol **80:**11265-73.

36. **Ng, M. L., J. Howe, V. Sreenivasan, and J. J. Mulders.** 1994. Flavivirus West Nile (Sarafend) egress at the plasma membrane. Arch Virol **137:**303-13.

37. **Ng, M. L., S. H. Tan, and J. J. Chu.** 2001. Transport and budding at two distinct sites of visible nucleocapsids of West Nile (Sarafend) virus. J Med Virol **65:**758-64.

38. **Niwa, H., K. Yamamura, and J. Miyazaki.** 1991. Efficient selection for high-expression transfectants with a novel eukaryotic vector. Gene **108:**193-9.

39. **Pessin, J. E., and M. Glaser.** 1980. Budding of Rous sarcoma virus and vesicular stomatitis virus from localized lipid regions in the plasma membrane of chicken embryo fibroblasts. J Biol Chem **255:**9044-50.

40. **Pitha, J., T. Irie, P. B. Sklar, and J. S. Nye.** 1988. Drug solubilizers to aid pharmacologists: amorphous cyclodextrin derivatives. Life Sci **43:**493-502.

41. **Rahman, S., T. Matsumura, K. Masuda, K. Kanemura, and T. Fukunaga.** 1998. Maturation site of dengue type 2 virus in cultured mosquito C6/36 cells and Vero cells. Kobe J Med Sci **44:**65-79.

42. **Rouser, G., G. Galli, and G. Kritchevsky.** 1967. Lipid composition of the normal human brain and its variations during various diseases. Pathol Biol **15:**195-200.

43. **Sakamoto, H., K. Okamoto, M. Aoki, H. Kato, A. Katsume, A. Ohta, T. Tsukuda, N. Shimma, Y. Aoki, M. Arisawa, M. Kohara, and M. Sudoh.** 2005. Host sphingolipid biosynthesis as a target for hepatitis C virus therapy. Nat Chem Biol **1:**333-7.

44. **Sato, K., H. Okamoto, S. Aihara, Y. Hoshi, T. Tanaka, and S. Mishiro.** 1993. Demonstration of sugar moiety on the surface of hepatitis C virions recovered from the circulation of infected humans. Virology **196:**354-7.

45. **Serafino, A., M. B. Valli, F. Andreola, A. Crema, G. Ravagnan, L. Bertolini, and G. Carloni.** 2003. Suggested role of the Golgi apparatus and endoplasmic reticulum for crucial sites of hepatitis C virus replication in human lymphoblastoid cells infected in vitro. J Med Virol **70:**31-41.

46. **Shi, S. T., K. J. Lee, H. Aizaki, S. B. Hwang, and M. M. Lai.** 2003. Hepatitis C virus RNA replication occurs on a detergent-resistant membrane that cofractionates

with caveolin-2. J Virol **77:**4160-8.

47. **Shinitzky, M., and M. Inbar.** 1976. Microviscosity parameters and protein mobility in biological membranes. Biochim Biophys Acta **433:**133-49.

48. **Shirakura, M., K. Murakami, T. Ichimura, R. Suzuki, T. Shimoji, K. Fukuda, K. Abe, S. Sato, M. Fukasawa, Y. Yamakawa, M. Nishijima, K. Moriishi, Y. Matsuura, T. Wakita, T. Suzuki, P.M. Howley, T. Miyamura, and I. Shoji.** 2007. E6AP ubiquitin ligase mediates ubiquitylation and degradation of hepatitis C virus core protein. J Virol **81**: 1174-85.

49. **Stuart, A. D., H. E. Eustace, T. A. McKee, and T. D. Brown.** 2002. A novel cell entry pathway for a DAF-using human enterovirus is dependent on lipid rafts. J Virol **76**: 9307-22.

50. **Takikawa, S., K. Ishii, H. Aizaki, T. Suzuki, H. Asakura, Y. Matsuura, and T. Miyamura.** 2000. Cell fusion activity of hepatitis C virus envelope proteins. J Virol **74:**5066-74.

51. **Tani, H., Y. Komoda, E. Matsuo, K. Suzuki, I. Hamamoto, T. Yamashita, K. Moriishi, K. Fujiyama, T. Kanto, N. Hayashi, A. Owsianka, A. H. Patel, M. A. Whitt, and Y. Matsuura.** 2007. Replication-competent recombinant vesicular stomatitis virus encoding hepatitis C virus envelope proteins. J Virol **81:**8601-12.

52. **Umehara, T., M. Sudoh, F. Yasui, C. Matsuda, Y. Hayashi, K. Chayama, and M. Kohara.** 2006. Serine palmitoyltransferase inhibitor suppresses HCV replication in a mouse model. Biochem Biophys Res Commun **346,** 67-73.

53. **Voisset, C., M. Lavie, F. Helle, A. O. De Beeck, A. Bilheu, J. Bertrand-Michel, F. Tercé, L. Cocquerel, C. Wychowski, N. Vu-Dac, and J. Dubuisson.** 2007. Ceramide enrichment of the plasma membrane induces CD81 internalization and inhibits hepatitis C virus entry. Cell Microbiol **10**:606-17.

54. **Wakita, T., T. Pietschmann, T. Kato, T. Date, M. Miyamoto, Z. Zhao, K. Murthy, A. Habermann, H. G. Krausslich, M. Mizokami, R. Bartenschlager, and T. J. Liang.** 2005. Production of infectious hepatitis C virus in tissue culture from a cloned viral genome. Nat Med **11:**791-6.

55. **Yasuda, S., H. Kitagawa, M. Ueno, H. Ishitani, M. Fukasawa, M. Nishijima, S. Kobayashi, and K. Hanada.** 2001. A novel inhibitor of ceramide trafficking from the endoplasmic reticulum to the site of sphingomyelin synthesis. J Biol Chem **276:**43994-4002.

56. **Zhong, J., P. Gastaminza, G. Cheng, S. Kapadia, T. Kato, D. R. Burton, S. F. Wieland, S. L. Uprichard, T. Wakita, and F. V. Chisari.** 2005. Robust hepatitis C virus infection in vitro. Proc Natl Acad Sci U S A **102:**9294-9

FIGURE LEGENDS

FIG. 1. Role of HCV-associated cholesterol in infection. (**A**) Effect of cholesterol depletion on HCV infectivity. HCVcc particles (~2 fmol of the core protein) were treated with B-CD at 0.1, 1, and 5 mg/ml for 1 h at 37°C. After removal of B-CD, Huh-7 cells were infected with the treated virus particles, after which the core protein content of infected cells at 72 h p.i. was determined as an indicator of infectivity, as previously established (*24*). (**B**) Effect of cholesterol replenishment on infectivity. After treatment with 5 mg/ml B-CD, virus was treated with medium alone or medium containing exogenous cholesterol for 1 h at 37°C. (**C**) Effect of cholesterol depletion and replenishment on density gradient profiles of the viral particles. The HCVcc treated with 5 mg/ml B-CD was replenished with exogenous cholesterol (1 mM), followed by being separated by 10-60% sucrose gradient ultracentrifugation. The core protein in each fraction was measured. Density of each fraction was determined by refractive index measurement. (D) Effect of cholesterol depletion and replenishment on viral infectivity. Each fraction (shown in panel C) was subjected to infection, and then the core proteins in the cells were measured at 72 h p.i. (**E**) Effect of cholesterol depletion on the infectivity of HCVpv (genotype 1a; gray bars) or control VSVdelG-GFP/G (black bars). The viruses were preincubated with B-CD for 1 h at 37°C before infection. (**F**) Left; culture medium from HCVcc producing cells was fractionated as above. For each fraction, the amounts of core and infectivity (intracellular core) are plotted. Peaks of the core (arrow) and infectivity (arrowhead) were indicated. Middle; an aliquot of fraction 8 (peak of the core; left panel) was treated with 1 mM cholesterol for 1 h at 37°C. The resultant and non-treated aliquot of the fraction were subjected to the sucrose gradient ultracentrifugation. The core in each fraction was plotted. Right; infectivity of fraction 6 and 8, as depict in the left, with or without cholesterol

treatment was determined as shown above. Columns and bars represent the mean and standard deviation of 4 independent experiments.

FIG. 2. Effect of sphingomyelin hydrolysis on viral infectivity. (**A**) Effect on the infectivity of HCVcc. HCVcc was treated with 0.1, 1 and 10 U/ml SMase for 1 h at 37°C, followed by removal of SMase by ultracentifugation. Huh-7 cells were infected with the treated virus, after which the core protein content of infected cells was determined at 72 h p.i. (**B**) Effect on the infectivity of HCVpv (genotype 1a; gray bars) or control VSVdelG-GFP/G (black bars). The viruses were preincubated with SMase for 1 h at 37°C before infection. Columns and bars represent the mean and standard deviation of four independent experiments.

FIG. 3. Effects of B-CD or SMase on virus attachment and internalization. (**A**) Virus attachment to Huh-7 cells was determined at 4°C after treatment of HCVcc with B-CD (1 and 5 mg/ml) or SMase (1 and 10 U/ml). An antibody against CD81 was used to ensure that the antibody did not inhibit HCVcc binding (7, 33). Heparinase was used to Viral RNA copies in the mock treatment sample (-) were normalized to total cellular RNA and arbitrarily set at 100%.

(**B**) Virus internalization was measured in Huh7-25, which is a CD81-negative subclone (CD81-)(3), and Huh7-25-CD81, which stably expresses CD81 (CD81+) after treatment of the virions with B-CD or SMase. After internalization for 2 h at 37°C, cells were exposed to trypsin (trypsin +) or to PBS (trypsin -). Huh7-25 was used to ensure that surface-bound virus would be removed by trypsin treatment. The amounts of HCV RNA in Huh7-25 and Huh7-25-CD81 cells infected with untreated HCVcc were assigned the arbitrary value of 100%, respectively. Results are representative of four independent experiments.

FIG. 4. Compartmentation of HCV structural proteins within DRM fractions. Lysates of HCVcc-infected cells infected with HCVcc were treated with 1% TX100 on ice, 1% TX100 at 37°C, or left untreated, followed by sucrose gradient centrifugation. For each fraction, the amount of core protein was determined by ELISA (**A**), and E1, calnexin, and caveolin-2 were analyzed by Western blotting (**B**). The amounts of core protein in each lysate (TX100, 37°C; TX100, 4°C; Untreated) were assigned the arbitrary value of 100%, respectively. (**C**) The lysates of 293T cells expressing HCV E1 or E2 protein were treated with 1% TX-100 on ice, 1% TX-100 at 37°C, or left untreated, followed by discontinuous sucrose gradient centrifugation. Each fraction was concentrated in a Centricon YM-30 filter unit and subjected to 12.5% SDS-PAGE, followed by immunoblotting with antibodies against calnexin, caveolin-2, Myc (E1), or FLAG (E2). (**D**) Upper; structures of HCV envelope genes used. Numbers indicated are aa positions of HCV. Signal sequence, transmembrane (TM) and cytoplasmic tail (CT) domains of VSV G protein are shown. Lower; the cell lysates expressing chimeric HCV E1 or E2 protein were treated with 1% TX-100 on ice or left untreated, followed by discontinuous sucrose gradient centrifugation. It has been reported that VSV-G is not associated with lipid (39). Calnexin, caveolin-2 , and chimertic glycoproteins (chimeric E1 and chimeric E2) were analyzed by immunoblotting. Fractions are numbered from 1 to 9 in order from top to bottom (light to heavy). M. membrane; NM, non membrane; DRM, detergent resistant membrane; DS, detergent soluble.

FIG. 5. Effects of B-CD- or SMase treatment of cells on HCV infectivity. Huh-7 cells were treated with B-CD at 0, 0.1, 1 and 5 mg/ml (**A**) and SMase at 0, 0.1, 1 and 10 U/ml (**B**) prior to HCVcc infection. Intracellular core levels were quantitated 72 h p.i. Columns represent the mean and standard deviation of 4 independent experiments.

FIG. 6. Anti-HCV effect of inhibitors of the sphingolipid biosynthetic pathway. Subgenomic replicon cells derived from the HCV isolates N or JFH-1, as well as HCVcc-producing cells, were treated with of ISP-1 (0.1, 1, 10 μM), HPA-12 (0.1, 1, 10 μM) or IFN-a (100 U/ml), for 72 h. HCV RNA titers in the replicon cells (**A**), as well as HCV core protein content within the culture medium of infected cells (**C**), were determined. Columns and bars represent the mean and standard deviation of four independent experiments. (**B**) De novo synthesis of sphingolipid in the absence or presence of ISP-1 (10 μM) and HPA-12 (10 μM) was monitored in duplicate by metabolic labeling with [^{14}C]serine for 2 h at 37°C. Cer, ceramide; PE, phosphatidylethanolamine; PS, phosphatidylserine; and SM, sphingomyelin.

TABLE 1. Cholesterol and phospholipid contents in HCVcc and cells

	[nmol/mg protein]		
	Cholesterol (Chol)	Phospholipids (PL)	Chol/PL
Cells, non-infected	105.9 ± 10.4	253.2 ± 10.6	0.42
Cells, JFH-1-infected	116.5 ± 10.0	292.0 ± 18.4	0.40
Virus, JFH-1	43.6 ± 2.4	33.8 ± 1.8	1.29
Virus, J6/JFH-1	28.7 ± 4.8	22.7 ± 2.9	1.26

Average values of 3 independent measurements with standard deviations are presented.

TABLE 1

TABLE 2. Depletion of virion-associated cholesterol by B-CD

Treatment	Radioactivity		Average (%)
	Exp 1	Exp 2	
No treatment	5327	5573	5450 (100)
B-CD (5 mg/ml)	3643	1646	2644 (48.5)

Radioactivities (cpm) of HCVcc samples were determined by subtracting that of non-infected cells from that of HCVcc-infected cells, in two experiments (Exp 1 and 2). Average of the data and % values relative to non-treated sample were indicated.

TABLE 2

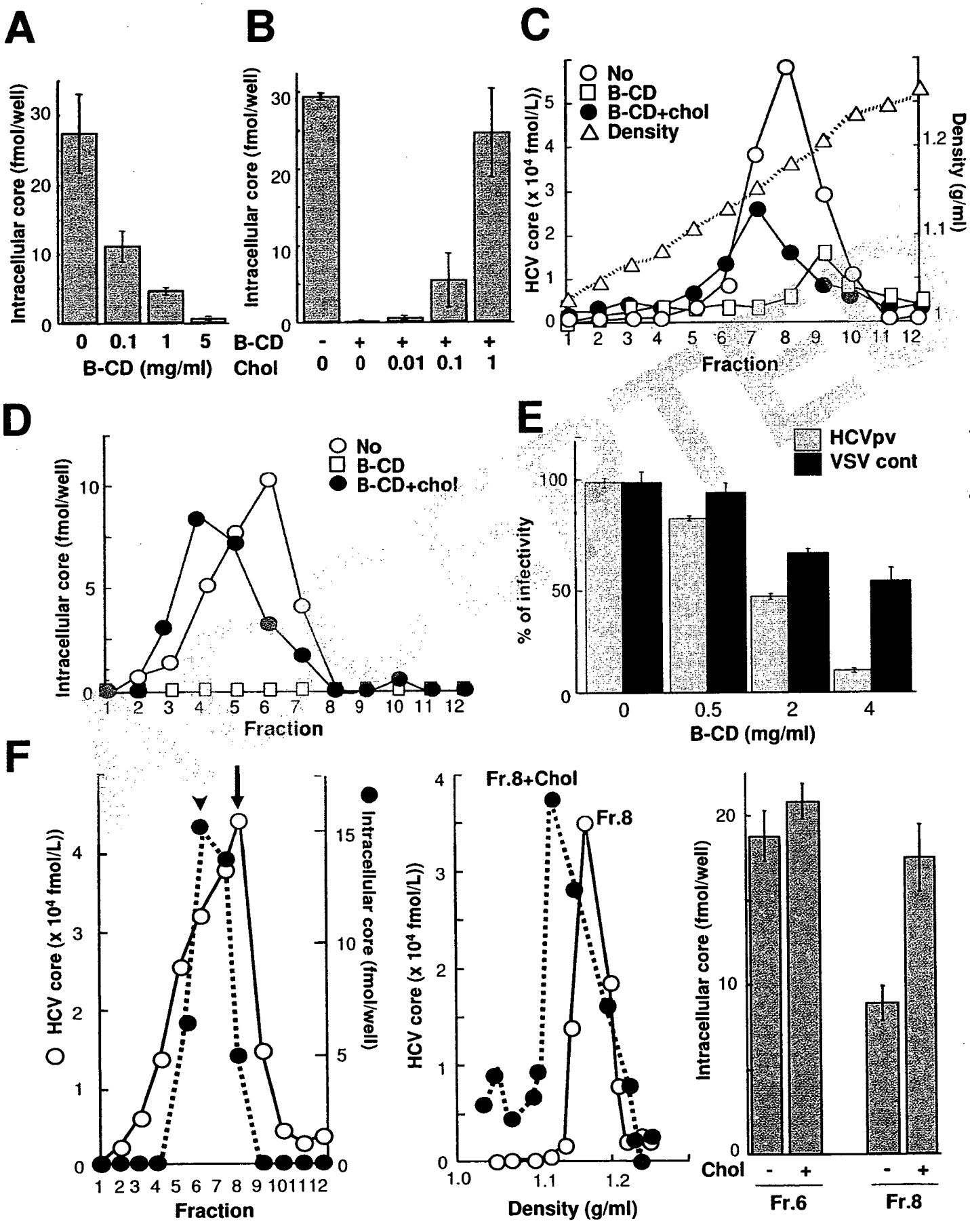
A
Intracellular core (fmol/well)
0 10 20 30
0 0.1 1 5
B-CD (mg/ml)
B
Intracellular core (fmol/well)
0 10 20 30
B-CD - + + + +
Chol 0 0 0.01 0.1 1
C
No
B-CD
B-CD+chol
Density
HCV core (x 10⁴ fmol/L)
Density (g/ml)
1 2 3 4 5 6 7 8 9 10 11 12
Fraction
D
No
B-CD
B-CD+chol
Intracellular core (fmol/well)
0 5 10
1 2 3 4 5 6 7 8 9 10 11 12
Fraction
E
HCVpv
VSV cont
% of infectivity
0 50 100
0 0.5 2 4
B-CD (mg/ml)
F
HCV core (x 10⁴ fmol/L)
Intracellular core (fmol/well)
1 2 3 4 5 6 7 8 9 10 11 12
Fraction
Fr.8+Chol
Fr.8
HCV core (x 10⁴ fmol/L)
1.0 1.1 1.2
Density (g/ml)
Intracellular core (fmol/well)
0 10 20
Chol - + - +
Fr.6 Fr.8

FIG. 1

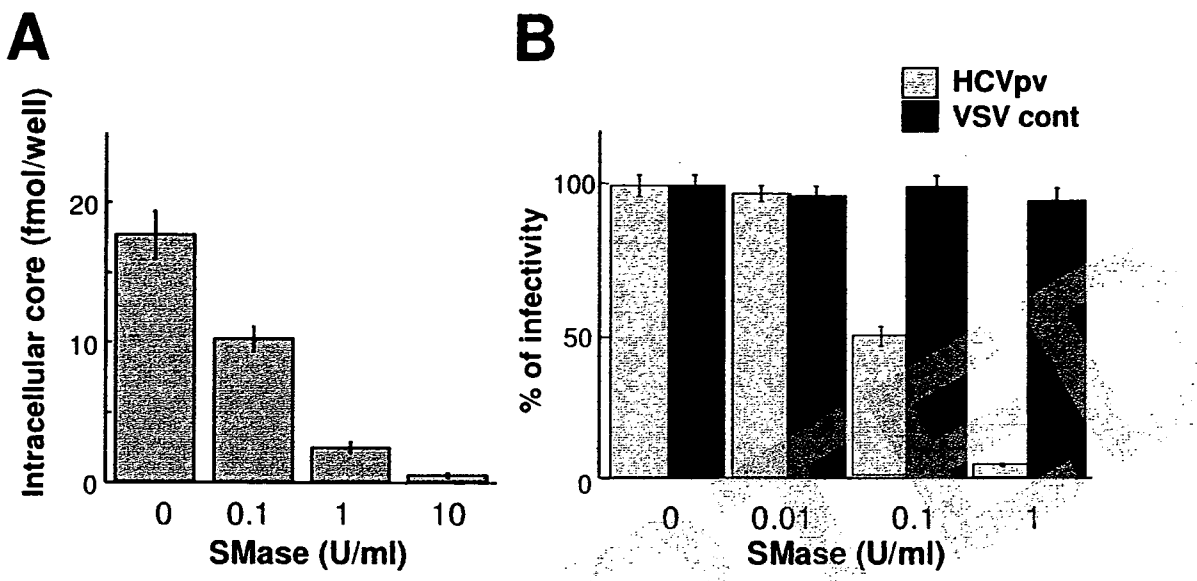
A
Intracellular core (fmol/well)
20
10
0
0
0.1
1
10
SMase (U/ml)
B
HCVpv
VSV cont
% of infectivity
100
50
0
0
0.01
0.1
1
SMase (U/ml)

FIG. 2

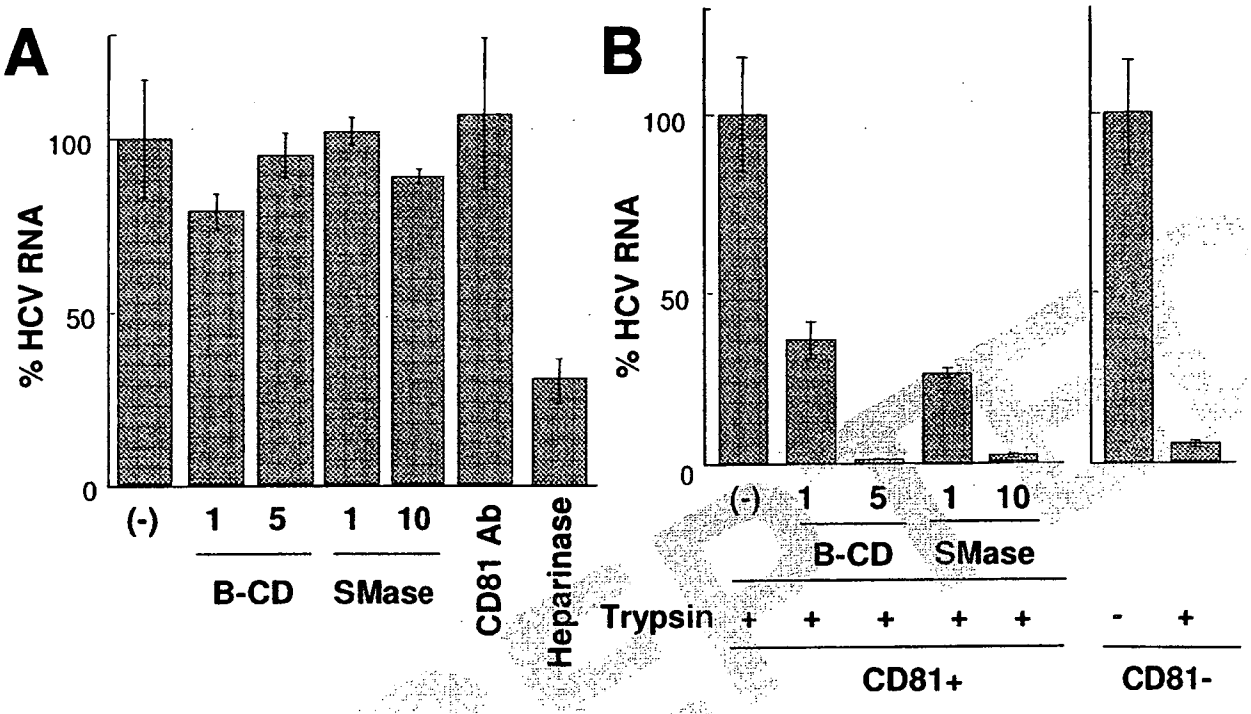
A
% HCV RNA
100
50
0
(-)
1
5
1
10
B-CD
SMase
CD81 Ab
Heparinase
B
% HCV RNA
100
50
0
(-)
1
5
1
10
B-CD
SMase
Trypsin
+
+
+
+
+
-
+
CD81+
CD81-

FIG. 3

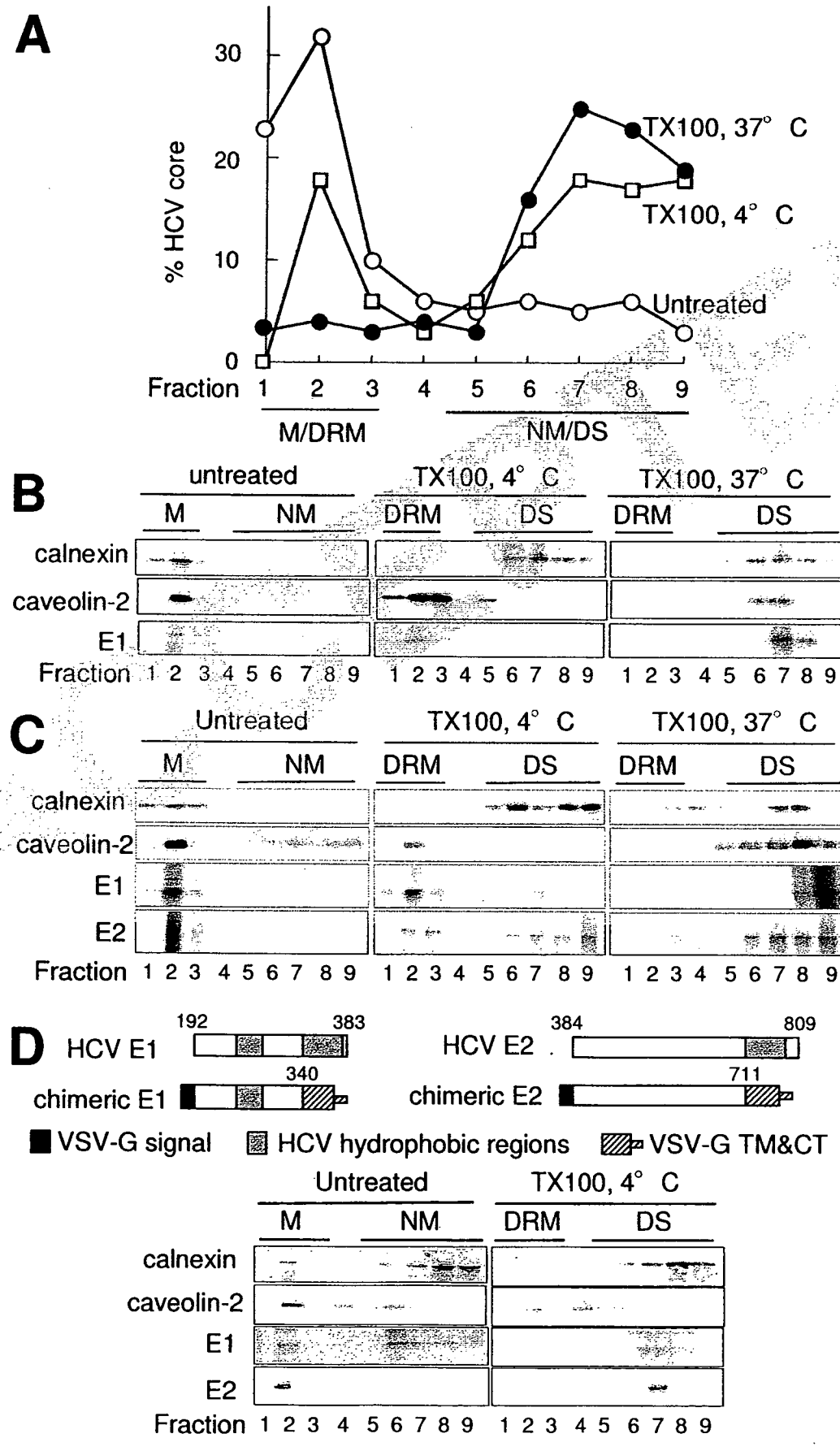
A
30
20
10
0
% HCV core
TX100, 37° C
TX100, 4° C
Untreated
Fraction 1 2 3 4 5 6 7 8 9
M/DRM
NM/DS
B
untreated
TX100, 4° C
TX100, 37° C
M
NM
DRM
DS
DRM
DS
calnexin
caveolin-2
E1
Fraction 1 2 3 4 5 6 7 8 9 1 2 3 4 5 6 7 8 9 1 2 3 4 5 6 7 8 9
C
Untreated
TX100, 4° C
TX100, 37° C
M
NM
DRM
DS
DRM
DS
calnexin
caveolin-2
E1
E2
Fraction 1 2 3 4 5 6 7 8 9 1 2 3 4 5 6 7 8 9 1 2 3 4 5 6 7 8 9
D
HCV E1
192
383
HCV E2
384
809
chimeric E1
340
chimeric E2
711
VSV-G signal
HCV hydrophobic regions
VSV-G TM&CT
Untreated
TX100, 4° C
M
NM
DRM
DS
calnexin
caveolin-2
E1
E2
Fraction 1 2 3 4 5 6 7 8 9 1 2 3 4 5 6 7 8 9

FIG. 4

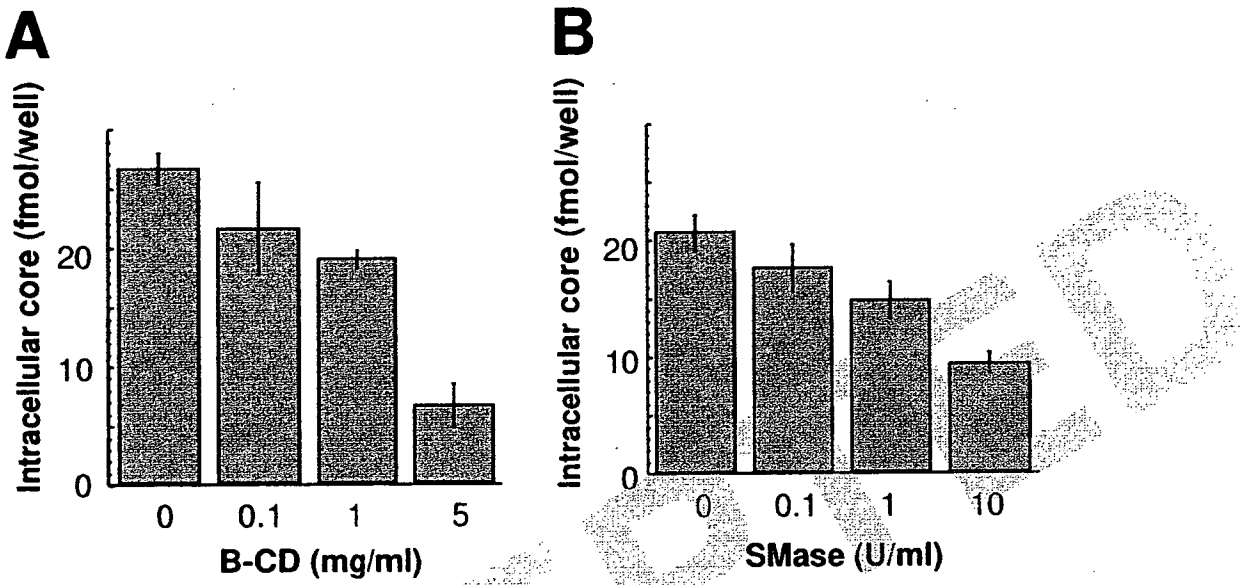

FIG. 5

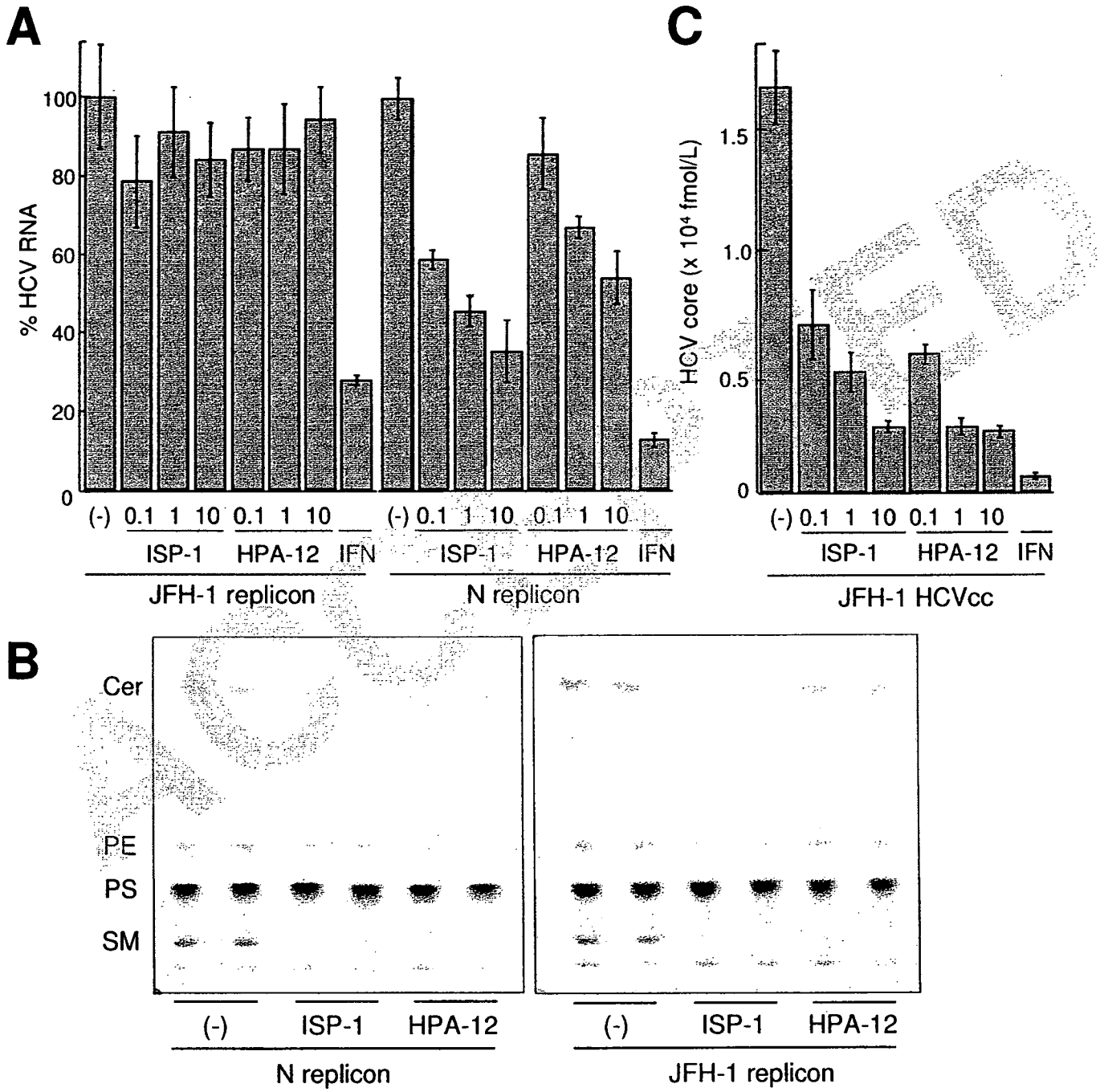
A
% HCV RNA
100
80
60
40
20
0
(-) 0.1 1 10 0.1 1 10
ISP-1
HPA-12
IFN
JFH-1 replicon
(-) 0.1 1 10 0.1 1 10
ISP-1
HPA-12
IFN
N replicon
C
HCV core (x 10⁴ fmol/L)
1.5
1.0
0.5
0
(-) 0.1 1 10 0.1 1 10
ISP-1
HPA-12
IFN
JFH-1 HCVcc
B
Cer
PE
PS
SM
(-)
ISP-1
HPA-12
N replicon
(-)
ISP-1
HPA-12
JFH-1 replicon

FIG. 6

JOURNAL OF VIROLOGY, Feb. 2007, p. 1174–1185 Vol. 81, No. 3
0022-538X/07/$08.00+0 doi:10.1128/JVI.01684-06

E6AP Ubiquitin Ligase Mediates Ubiquitylation and Degradation of Hepatitis C Virus Core Protein▽

Masayuki Shirakura,[1] Kyoko Murakami,[1] Tohru Ichimura,[2] Ryosuke Suzuki,[1] Tetsu Shimoji,[1] Kouichirou Fukuda,[1] Katsutoshi Abe,[1] Shigeko Sato,[3] Masayoshi Fukasawa,[3] Yoshio Yamakawa,[3] Masahiro Nishijima,[3] Kohji Moriishi,[4] Yoshiharu Matsuura,[4] Takaji Wakita,[1] Tetsuro Suzuki,[1] Peter M. Howley,[5] Tatsuo Miyamura,[1] and Ikuo Shoji[1]*

Department of Virology II[1] and Department of Biochemistry and Cell Biology,[3] National Institute of Infectious Diseases, Shinjuku-ku, Tokyo 162-8640, Japan; Department of Chemistry, Graduate School of Science, Tokyo Metropolitan University, Hachioji-shi, Tokyo 192-0397, Japan[2]; Department of Molecular Virology, Research Institute for Microbial Diseases, Osaka University, Osaka 565-0871, Japan[4]; and Department of Pathology, Harvard Medical School, 77 Avenue Louis Pasteur, Boston, Massachusetts 02115[5]

Received 4 August 2006/Accepted 8 November 2006

Hepatitis C virus (HCV) core protein is a major component of viral nucleocapsid and a multifunctional protein involved in viral pathogenesis and hepatocarcinogenesis. We previously showed that the HCV core protein is degraded through the ubiquitin-proteasome pathway. However, the molecular machinery for core ubiquitylation is unknown. Using tandem affinity purification, we identified the ubiquitin ligase E6AP as an HCV core-binding protein. E6AP was found to bind to the core protein in vitro and in vivo and promote its degradation in hepatic and nonhepatic cells. Knockdown of endogenous E6AP by RNA interference increased the HCV core protein level. In vitro and in vivo ubiquitylation assays showed that E6AP promotes ubiquitylation of the core protein. Exogenous expression of E6AP decreased intracellular core protein levels and supernatant HCV infectivity titers in the HCV JFH1-infected Huh-7 cells. Furthermore, knockdown of endogenous E6AP by RNA interference increased intracellular core protein levels and supernatant HCV infectivity titers in the HCV JFH1-infected cells. Taken together, our results provide evidence that E6AP mediates ubiquitylation and degradation of HCV core protein. We propose that the E6AP-mediated ubiquitin-proteasome pathway may affect the production of HCV particles through controlling the amounts of viral nucleocapsid protein.

Hepatitis C virus (HCV; a single-stranded, positive-sense RNA virus that is classified in the family *Flaviviridae*) is the main cause of chronic hepatitis, liver cirrhosis, and hepatocellular carcinoma (5, 26, 45). More than 170 million people worldwide are chronically infected with HCV (41). The approximately 9.6-kb HCV genome encodes a unique open reading frame that is translated into a polyprotein (5, 54). The polyprotein is cleaved cotranslationally into at least 10 proteins by viral proteases and cellular signalases (6, 10).

The HCV core protein represents the first 1 to 191 amino acids (aa) of the polyprotein and is followed by two glycoproteins, E1 and E2 (6). The core protein plays a central role in the packaging of viral RNA (25, 40); modulates various cellular processes, including signal transduction pathways, transcriptional control, cell cycle progression, apoptosis, lipid metabolism, and the immune response (9, 40); and has transforming potential in certain cells (43). Mice transgenic for the HCV core gene develop steatosis (32) and later hepatocellular carcinoma (31). These findings suggest that HCV core protein plays a crucial role in hepatocarcinogenesis.

Two major forms of the HCV core protein, p21 (mature form) and p23 (immature form), can be generated in cultured cells (60). Cellular signal peptidase cleaves at the junction of the core/E1, releasing the immature form of the core protein from the polypeptide (12, 46). Signal peptide peptidase cleaves just before the signal sequence, liberating the mature form of the HCV core protein at the cytoplasmic face of the endoplasmic reticulum (29). Several different sites have been proposed as potential cleavage sites of signal peptide peptidase, such as Leu-179 (15, 29), Phe-177 (36, 37), Leu-182 (15), and Ser-173 (46). Further processing of the HCV core protein yields a 17-kDa product with a C terminus at around amino acid 152. A truncated form of the core protein, p17, was found in transfected cells (42, 52) and liver tissues from humans with hepatocellular carcinoma (59). The majority of this protein translocates to the nucleus. The C terminus of the core protein is important for regulating the stability of the protein (20, 52).

We previously showed that the C-terminally truncated forms of the core protein are degraded through the ubiquitin-proteasome pathway (52). We found that the mature form of the core protein, p21, also links to a few ubiquitin moieties, suggesting that the ubiquitin-proteasome pathway involves proteolysis of heterologous species of the core protein (52). Overexpression of PA28γ (a REG family proteasome activator also known as REGγ or Ki antigen) enhances the proteasomal degradation of the HCV core protein (30). A recent study has shown that

* Corresponding author. Mailing address: Department of Virology II, National Institute of Infectious Diseases, 1-23-1 Toyama, Shinjuku-ku, Tokyo 162-8640, Japan. Phone: 81 3-5285-1111. Fax: 81 3-5285-1161. E-mail: ishoji@nih.go.jp.

▽ Published ahead of print on 15 November 2006.

PA28γ is involved in the degradation of the steroid receptor coactivator 3 (SRC-3) in an ATP- and ubiquitin-independent manner (27). It is still unclear what E3 ubiquitin ligase is responsible for ubiquitylation of the HCV core protein.

E6AP was initially identified as the cellular factor that stimulates ubiquitin-mediated degradation of the tumor suppressor p53 in conjunction with the E6 protein of cancer-associated human papillomavirus types 16 and 18 (14, 48). The E6-E6AP complex functions as a E3 ubiquitin ligase in the ubiquitylation of p53 (49). E6AP is the prototype of a family of ubiquitin ligases called HECT domain ubiquitin ligases, all of which contain a domain *h*omologous to the *E6AP c*arboxyl *t*erminus (13). Interestingly, E6AP is not involved in the regulation of p53 ubiquitylation in the absence of E6 (55). Several potential E6-independent substrates for E6AP have been identified, such as hHR23A, Blk, and Mcm7 (23, 24, 35). E6AP is also a candidate gene for Angelman syndrome, which is a severe neurological disorder characterized by mental retardation (21).

This study aimed to identify endogenous ubiquitin-proteasome pathway proteins that are associated with HCV core protein. Tandem affinity purification and mass spectrometry analysis identified E6AP as an HCV core-binding protein. Here we present evidence that E6AP associates with HCV core protein in vitro and in vivo and is involved in ubiquitylation and degradation of HCV core protein. We propose that an E6AP-mediated ubiquitin-proteasome pathway may affect the production of HCV particles through controlling the amounts of HCV core protein.

MATERIALS AND METHODS

Cell culture and transfection. Human embryonic kidney 293T cells, human hepatoblastoma HepG2 cells, and human hepatoma Huh-7 cells were cultured in Dulbecco's modified Eagle's medium (Sigma) supplemented with 50 IU/ml penicillin, 50 μg/ml streptomycin (Invitrogen), and 10% (vol/vol) fetal bovine serum (JRH Biosciences) at 37°C in a 5% CO_2 incubator. 293T cells and HepG2 cells were transfected with plasmid DNA using FuGene 6 transfection reagents (Roche). Huh-7 cells were transfected with plasmid DNA using *Trans*IT LT1 transfection reagents (Mirus).

Plasmids and recombinant baculoviruses. MEF tag cassette (containing *m*yc tag, the tobacco *e*tch virus protease cleavage site, and *F*LAG tag) (16) was fused to the N terminus of the cDNA encoding core protein of HCV NIHJ1 (genotype 1b) (1). To express MEF-tagged core protein in mammalian cells, the genome coding for HCV core protein (amino acids 1 to 191) was amplified by PCR using pBR HCV NIHJ1 as a template. Sense oligonucleotide containing a Kozak consensus translation initiation codon and antisense oligonucleotide containing an in-frame translation stop codon were synthesized by PCR. The amplified PCR product was purified, digested with EcoRI and EcoRV, and then inserted into the EcoRI-EcoRV site of pcDNA3-MEF. FLAG-tagged HCV core expression plasmids based upon pCAGGS (34) were described previously (30). To express E6AP and the active-site cysteine-to-alanine mutant of E6AP in mammalian cells, pCMV4-HA-E6AP isoform II and pCMV4-HA-E6AP C-A were utilized (19). The C-A mutation was introduced at the site of E6AP C843. To express E6AP and E6AP C-A under the CAG promoter, the E6AP fragment and the E6AP C-A fragment were amplified by PCR, purified, digested with SmaI and NotI, and blunt ended using a DNA blunting kit (Takara). These PCR fragments were subcloned into pCAGGS.

To make a fusion protein consisting of glutathione *S*-transferase (GST) fused to the N terminus of E6AP in *Escherichia coli*, the E6AP fragment was amplified by PCR and the resultant product was cloned into the SmaI-NotI site of pGEX4T-1 vector (Amersham Biosciences). To express a series of E6AP truncation mutants as GST fusion proteins, each fragment was amplified by PCR and cloned into the SmaI-NotI site of pGEX4T-1. To purify GST core protein efficiently by two-step affinity purification, we fused hexahistidine (His) tag to the C terminus of GST fusion proteins. To bacterially express HCV core (aa 1 to 173) protein as a fusion protein containing N-terminal GST tag and C-terminal His tag, core fragment was amplified by PCR and the resultant product was cloned into the EcoRI-NotI site of pGEX4T-1 vector. The resultant plasmid was designated pGEX GST-C173HT. To express GST core (1–152)-His and GST-His in *E. coli*, pGEX core (1–152)-His and pGEX-His were constructed similarly. The resultant plasmids were designated pGEX GST-C152HT and pGEX GST-HT, respectively.

To generate recombinant baculoviruses expressing GST-E6AP, GST-E6AP fragment was excised from pGEX E6AP by digestion with SmaI and Tth111I and ligated into the SmaI-Tth111I site of pVL1392 (Invitrogen). To express GST-E6AP C-A, pVLGST-E6AP C-A was constructed similarly. To generate recombinant baculovirus expressing HCV core (aa 1 to 173) protein as a fusion protein containing N-terminal GST tag and C-terminal His tag, GST-C173HT fragment was amplified by PCR using pGEX GST-C173HT as a template, digested with BglII-XbaI, and subcloned into the BglII-XbaI site of pVL1392. To generate recombinant baculoviruses expressing GST-C152HT and GST-HT, cDNA fragments corresponding to GST-C152HT and GST-HT were amplified by PCR and subcloned into pVL1392, respectively. The resultant plasmids were designated pVLGST-C173HT, pVLGST-C152HT, and pVLGST-HT. To generate recombinant baculovirus expressing MEF-tagged E6AP, cDNA fragment encoding MEF-E6AP was subcloned into pVL1392. To express HCV core protein in the TNT-coupled wheat germ lysate system (Promega), HCV core cDNA was inserted in the EcoRI site of pCMVTNT (Promega). The primer sequences used in this study are available from the authors upon request. The sequences of the inserts were extensively verified using an ABI PRISM 3100-Avant Genetic Analyzer (Applied Biosystems). Recombinant baculoviruses were recovered using a BaculoGold transfection kit (Pharmingen) according to the manufacturer's instructions.

Antibodies. The mouse monoclonal antibodies (MAbs) used in this study were anti-hemagglutinin (anti-HA) MAb (12CA5; Roche), anti-FLAG (M2) MAb (Sigma), anti-c-*myc* MAb (9E10; Santa Cruz), anti-glyceraldehyde-3-phosphate dehydrogenase (anti-GAPDH) MAb (Chemicon), anti-GST MAb (Santa Cruz), anti-ubiquitin MAb (Chemicon), anti-E6AP MAb (E6AP-330) (Sigma), anticore MAb (B2; Anogen), and another anti-core MAb (2H9) (56). Polyclonal antibodies (PAbs) used in this study were anti-HA rabbit PAb (Y-11; Santa Cruz), anti-FLAG rabbit PAb (F7425; Sigma), anti-E6AP rabbit PAb (H-182; Santa Cruz), anti-DDX3 rabbit PAb (47), anti-PA28γ rabbit PAb (Affiniti), and anti-GST goat PAb (Amersham). Anticore rabbit PAb (TS1) was raised against the recombinant GST core protein.

MEF purification procedure. 293T cells were transfected with the plasmid expressing MEF core by the calcium phosphate precipitation method (4). After the cells were lysed, the expressed MEF core and its binding proteins were recovered following the procedure described previously (16). 293T cells transfected with pcDNA3-MEF core in four 10-cm dishes were lysed in 2 ml of lysis buffer: 50 mM Tris-HCl (pH 7.5), 150 mM NaCl, 10% (wt/vol) glycerol, 100 mM NaF, 1 mM Na_3VO_4, 1% (wt/vol) Triton X-100, 5 μM $ZnCl_2$, 2 mM phenylmethylsulfonyl fluoride, 10 μg/ml aprotinin, and 1 μg/ml leupeptin. The lysate was centrifuged at 100,000 × *g* for 20 min at 4°C. The supernatant was passed through a 5-μm filter, incubated with 100 μl of Sepharose beads for 60 min at 4°C, and then passed through a 0.65-μm filter. The filtered supernatant was mixed with 100 μl of anti-myc-conjugated Sepharose beads for the first immunoprecipitation. After incubation for 90 min at 4°C, the beads were washed five times with 1 ml of TNTG buffer (20 mM Tris-HCl, pH 7.5, 150 mM NaCl, 10% [wt/vol] glycerol, and 1% [wt/vol] Triton X-100), twice with 1 ml of buffer A (20 mM Tris-HCl, pH 7.5, 150 mM NaCl, and 1% [wt/vol] Triton X-100), and finally once with 1 ml of TNT buffer (50 mM Tris-HCl, pH 8.0, 150 mM NaCl, 1% [wt/vol] Triton X-100). The washed beads were incubated with 10 U of tobacco etch virus protease (Invitrogen) in TNT buffer (100 μl) to release bound protein complexes from the beads. After incubation for 60 min at room temperature, the supernatant was pooled and the beads were washed twice with 70 μl of buffer A. The resulting supernatants were combined and incubated with 12 μl of FLAG-Sepharose beads for the second immunoprecipitation. After incubation for 60 min at room temperature, the beads were washed three times with 240 μl of buffer A, and proteins bound to the immobilized HCV core protein on the FLAG beads were dissociated by incubation with 80 μg/ml FLAG peptide (NH_2-Asp-Tyr-Lys-Asp-Asp-Asp-Asp-Lys-COOH) (Sigma).

MS/MS. Proteins were separated by 9% sodium dodecyl sulfate-polyacrylamide gel electrophoresis (SDS-PAGE) and visualized by silver staining. The stained bands were excised and digested in the gel with lysylendoprotease-C (Lys-C), and the resulting peptide mixtures were analyzed using a direct nanoflow liquid chromatography-tandem mass spectrometry (MS/MS) system (33), equipped with an electrospray interface reversed-phase column, a nanoflow gradient device, a high-resolution Q-time of flight hybrid mass spectrometer (Q-TOF2; Micromass), and an automated data analysis system. All the MS/MS

spectra were searched against the nonredundant protein sequence database maintained at the National Center for Biotechnology Information using the Mascot program (Matrixscience) to identify proteins. The MS/MS signal assignments were also confirmed manually.

Expression and purification of recombinant proteins. *E. coli* BL21(DE3) cells were transformed with plasmids expressing GST fusion protein or His-tagged protein and grown at 37°C. Expression of the fusion protein was induced by 1 mM isopropyl-β-D-thiogalactopyranoside at 37°C for 4 h. Bacteria were harvested, suspended in lysis buffer (phosphate-buffered saline [PBS] containing 1% Triton X-100), and sonicated on ice.

Hi5 cells were infected with recombinant baculoviruses to produce GST-C173HT, GST-C152HT, GST-HT, MEF-E6AP, and His-tagged mouse E1 (17). GST and GST fusion proteins were purified on glutathione-Sepharose beads (Amersham Bioscience) according to the manufacturer's protocols. His-tagged proteins were purified on nickel-nitrilotriacetic acid beads (QIAGEN) according to the manufacturer's protocols. MEF-E6AP and MEF-E6AP C-A were purified on anti-FLAG M2 agarose beads (Sigma) according to the manufacturer's protocols.

Immunoblot analysis. Immunoblot analysis was performed essentially as described previously (11). The membrane was visualized with SuperSignal West Pico chemiluminescent substrate (Pierce).

HCV core protein and E6AP binding assays. To map the E6AP binding site on HCV core protein, 2.5 μg of purified recombinant GST-E6AP expressed in Hi5 cells was mixed with 1,000 μg of 293T cell lysates transfected with a series of FLAG-tagged HCV core deletion mutants as indicated. The protein concentration of the cells was determined using the bicinchoninic acid protein assay kit (Pierce). The mixtures were immunoprecipitated with anti-FLAG M2 agarose beads (Sigma), and proteins bound to the immobilized HCV core protein on anti-FLAG beads were dissociated with FLAG peptide (Sigma). The eluates were analyzed by immunoblotting with anti-GST PAb. To map the HCV core-binding site on E6AP, GST pull-down assays were performed as described previously (51).

In vivo ubiquitylation assay. In vivo ubiquitylation assays were performed essentially as described previously (57). FLAG-core was immunoprecipitated with anti-FLAG beads. Immunoprecipitates were analyzed by immunoblotting, using either anti-HA PAb or anticore PAb (TS1) to detect ubiquitylated core proteins.

In vitro ubiquitylation assay. For in vitro ubiquitylation of HCV core protein, purified GST-C173HT and GST-C152HT were used as substrates. Purified GST-HT was used as a negative control. Assays were done in 40-μl volumes containing 20 mM Tris-HCl, pH 7.6, 50 mM NaCl, 5 mM ATP, 10 mM $MgCl_2$, 8 μg of bovine ubiquitin (Sigma), 0.1 mM dithiothreitol, 200 ng mouse E1, 200 ng E2 (UbcH7), and 0.5 μg each of MEF-E6AP or MEF-E6AP C-A. The reaction mixtures were incubated at 37°C for 120 min followed by purification with glutathione-Sepharose beads and immunoblotting with the indicated antibodies.

siRNA transfection. 293T cells or Huh-7 cells at 3×10^5 cells in a six-well plate were transfected with 40 pmol of either E6AP-specific short interfering RNA (siRNA; Sigma) or scramble negative-control siRNA duplexes (Sigma) using HiPerFect transfection reagent (QIAGEN) following the manufacturer's instructions. The siRNA target sequences were as follows: E6AP (sense), 5′-GGGUC UACACCAGAUUGCUTT-3′; scramble negative control (sense), 5′-UUGCG GGUCUAAUCACCGATT-3′.

CHX half-life experiments. To examine the half-life of HCV core protein, transfected 293T cells were treated with 50 μg/ml cycloheximide (CHX) at 44 h posttransfection. The cells at zero time points were harvested immediately after treatment with CHX. Cells from subsequent time points were incubated in medium containing CHX at 37°C for 3, 6, and 9 h as indicated.

Infection of Huh-7 cells with secreted HCV. Infectious HCV JFH1 was produced in Huh-7.5.1 cells (61) as described previously (56). Culture supernatant containing infectious HCV JFH1 was collected and passed through a 0.22-μm filter. Naïve Huh-7 cells were seeded 24 h before infection at a density of 1×10^6 in a 10-cm dish. The cells were incubated with 2.5 ml of the inoculum (6.5×10^3 50% tissue culture infectious dose [$TCID_{50}$]/ml) for 3 h, washed three times with PBS, and supplemented with fresh complete Dulbecco's modified Eagle's medium. Then the cells were transfected with 6 μg each of pCAGGS, pCAG-HA-E6AP, or pCAG-HA-E6AP C-A by using TransIT LT1 (Mirus). The cells were trypsinized and replated in six-well plates at 1 day postinfection. The culture medium was changed every 2 days. The culture supernatants and the cells were collected at days 3 and 7 postinfection.

Quantitation of HCV RNA and core protein. We quantitated HCV core protein in cell lysate using the HCV core antigen enzyme-linked immunosorbent assay (ELISA) (Ortho-Clinical Diagnostics). Total RNA was extracted from cells using TRIzol reagent (Invitrogen). To quantitate HCV RNAs, real-time reverse transcription-PCR was performed as described previously (53).

Infectivity assay. The $TCID_{50}$ was calculated essentially based on the method described previously (28). Virus titration was performed by seeding Huh-7 cells in 96-well plates at 1×10^4 cells/well. Samples were serially diluted fivefold in complete growth medium and used to infect the seeded cells (six wells per dilution). Following 3 days of incubation, the cells were immunostained for core with anticore MAb (2H9). Wells that expressed at least one core-expressing cell were counted as positive, and the $TCID_{50}$ was calculated.

Immunocytochemistry and fluorescence microscopy. Cells on collagen-coated coverslips were washed with PBS, fixed with 4% paraformaldehyde for 30 min at 4°C, and permeabilized with PBS containing 0.2% Triton X-100. Cells were preincubated with BlockAce (Dainippon Pharmaceuticals), incubated with specific antibodies as primary antibodies, washed, and incubated with rhodamine-conjugated goat anti-rabbit immunoglobulin G (ICN Pharmaceuticals, Inc.) and Qdot 565-conjugated goat anti-mouse immunoglobulin G (Quantumdot) as secondary antibody. Then the cells were washed with PBS, counterstained with DAPI (4′,6′-diamidino-2-phenylindole) solution (Sigma) for 3 min, mounted on glass slides, and examined with a BZ-8000 microscope (Keyence).

Knockdown of endogenous E6AP in HCV JFH1-infected Huh-7 cells. Naïve Huh-7 cells at 10^6 cells/10-cm dish were inoculated with 2.5 ml of the inoculum including infectious HCV JFH1 (6.5×10^3 $TCID_{50}$/ml) and cultured. The cells were replated in a six-well plate at 3×10^5 cells/well at day 11 postinfection and transfected with 40 pmol of E6AP siRNA or control siRNA. The culture medium was changed at 24 h after transfection. The cells were harvested at day 2 after transfection, and the intracellular core protein levels were quantitated using the HCV core antigen ELISA. The culture supernatants were collected at day 2 after transfection and assayed for $TCID_{50}$ determinations.

RESULTS

Identification of E6AP as an HCV core-binding protein. To identify the molecular machinery for HCV core ubiquitylation, we searched for endogenous ubiquitin-proteasome pathway proteins that associated with HCV core protein. HCV core-binding proteins (i.e., MEF core and its binding proteins, recovered from lysed cells) were purified by a tandem affinity purification procedure using a tandem tag (known as MEF tag) (16). Ten proteins were reproducibly detected (Fig. 1A, lane 2), but none were recovered from lysed control cells transfected with empty vector alone (Fig. 1A, lane 1).

To identify the proteins, silver-stained bands were excised from the gel, digested by Lys-C, and analyzed using a direct nanoflow liquid chromatography-MS/MS system. Nine proteins were identified: two known HCV core-binding proteins, human DEAD box protein DDX3 (38) and proteasome activator PA28γ (30), and seven potential HCV core-binding proteins. E6AP was identified (Fig. 1A, lane 2) on the basis of five independent MS/MS spectra (Table 1). Immunoblot analyses confirmed the proteomic identification of E6AP, DDX3, PA28γ, and MEF-core (Fig. 1B to E).

E6AP binding domain for HCV core protein. The E6AP binding domain for HCV core protein was investigated. Figure 2A is a schematic representation of E6AP and known motifs in E6AP. A series of deletion mutants of E6AP as GST fusion proteins were expressed in *E. coli*. GST pull-down assays found that the carboxyl-terminal deletion mutant E6AP (1–517), but not E6AP (1–418) (Fig. 2C, lanes C and D), and the amino-terminal deletion mutant E6AP (418–875), but not E6AP (517–875) (Fig. 2C, lanes J and K), were able to bind to the core protein. The signal was absent when unprogrammed wheat germ extracts (the negative control) were used as a source of proteins (data not shown). GST pull-down assays (Fig. 2B) found that the region from aa 418 to aa 517 is important for binding to the HCV core protein. An assay of the

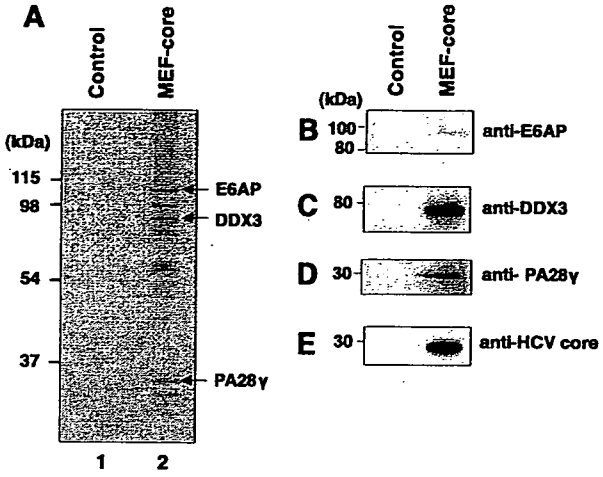

FIG. 1. HCV core protein associates with E6AP in vivo. (A) 293T cells were transfected with pcDNA3-MEF-core or empty plasmid, incubated for 48 h, and then harvested. The expressed MEF-core and binding proteins were recovered using the MEF purification procedure. Proteins bound to the MEF-core immobilized on anti-FLAG beads were dissociated with FLAG peptides, resolved by 9% SDS-PAGE, and visualized by silver staining. Control experiments were performed using 293T cells transfected with vector alone. The positions of E6AP, DDX3, and PA28γ are indicated by arrows. (B to E) The proteins detected in panel A were confirmed by immunoblotting with appropriate antibodies: E6AP (B), DDX3 (C), PA28γ (D), and MEF-core (E).

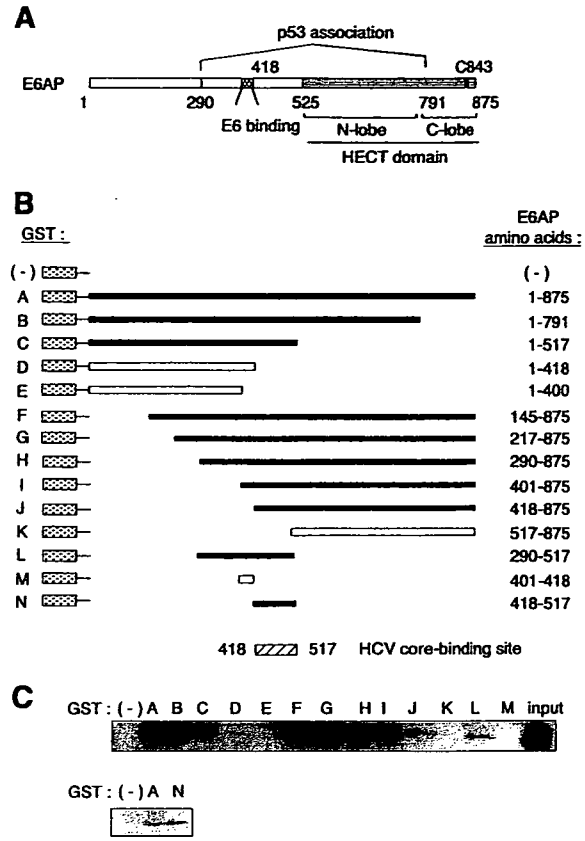

FIG. 2. Mapping of the HCV core-binding domain for E6AP. (A) Structure of E6AP. Shown is a schematic representation of the regions of E6AP isoform II that mediate E6 binding (aa 401 to 418), E6-dependent association with p53 (aa 290 to 791), and the HECT catalytic domain (aa 525 to 875). The catalytic cysteine residue is located at aa 843. (B) Schematic representation of GST-E6AP proteins. GST proteins A through N contain the E6AP amino acids indicated to the right. The shaded region of each represents the GST sequence. Closed boxes represent proteins that are bound specifically to HCV core protein, and open boxes represent those that are not bound. (C) Binding of HCV core protein to GST-E6AP proteins A through N. In vitro-translated core protein (aa 1 to 173) was assayed for association with GST (-) or the GST-E6AP fusion proteins A through N. Association of core protein was detected by immunoblotting with anti-core MAb.

ability of GST-E6AP (418–517) to bind to the HCV core protein was confirmatory (Fig. 2C, lane N) and led to the conclusion that the HCV core-binding domain of E6AP was aa 418 to aa 517.

The HCV core-binding domain for E6AP. By use of a panel of HCV core deletion mutants (Fig. 3A), GST-E6AP was found to coimmunoprecipitate with all of the FLAG-core proteins (Fig. 3A, lanes A to H) except FLAG-core (72–191) or FLAG-core (92–191) (Fig. 3A, lanes I and J). No association of control GST protein with any FLAG-core proteins was observed (data not shown). These data suggest that the aa-58-to-aa-71 segment of the HCV core binds to E6AP. The ability of GST-core (58–71) to associate with purified MEF-E6AP confirmed that the core (aa 58–71) was the site for E6AP binding on the HCV core protein (Fig. 3B).

E6AP decreases steady-state levels of HCV core protein in 293T cells and HepG2 cells. One of the features of HECT domain ubiquitin ligases is direct association with their substrates (50). Thus, we hypothesized that E6AP would function as an E3 ubiquitin ligase for the HCV core protein. We assessed the effects of E6AP on the HCV core protein in 293T cells. FLAG-core (1–191) together with HA-tagged wild-type E6AP, catalytically inactive mutant E6AP, E6AP C-A (19), or WWP1 (another HECT domain ubiquitin ligase) (22) was introduced into 293T cells, and the levels of the core protein were examined by immunoblotting. The steady-state levels of the core protein decreased with an increase in the amount of E6AP plasmids (Fig. 4A and B). However, neither E6AP C-A mutant nor WWP1 decreased the steady-state levels of the core protein, suggesting that E6AP enhances degradation of the core protein.

To verify the critical need for endogenous E6AP in the core degradation, expression of E6AP was knocked down by siRNA and the expression of the core protein and E6AP was assayed by immunoblotting. Transfection of the E6AP-specific siRNA

TABLE 1. Identification of E6AP by tandem mass spectrometry[a]

Peptide *m/z*	Sequence determined	Residues
720.9	VFSSAEALVQSFR	156–168
922.4	AACSAAAMEEDSEASSSR	196–213
774.9	MMETFQQLITYK	339–350
1,053.1	ITVLYSLVQGQQLNPYLR	507–524
809.4	EFVISYSDYILNK	712–724

[a] The protein was ubiquitin protein ligase E3A (E6AP) isoform 2 (GenBank accession no. NP_000453).

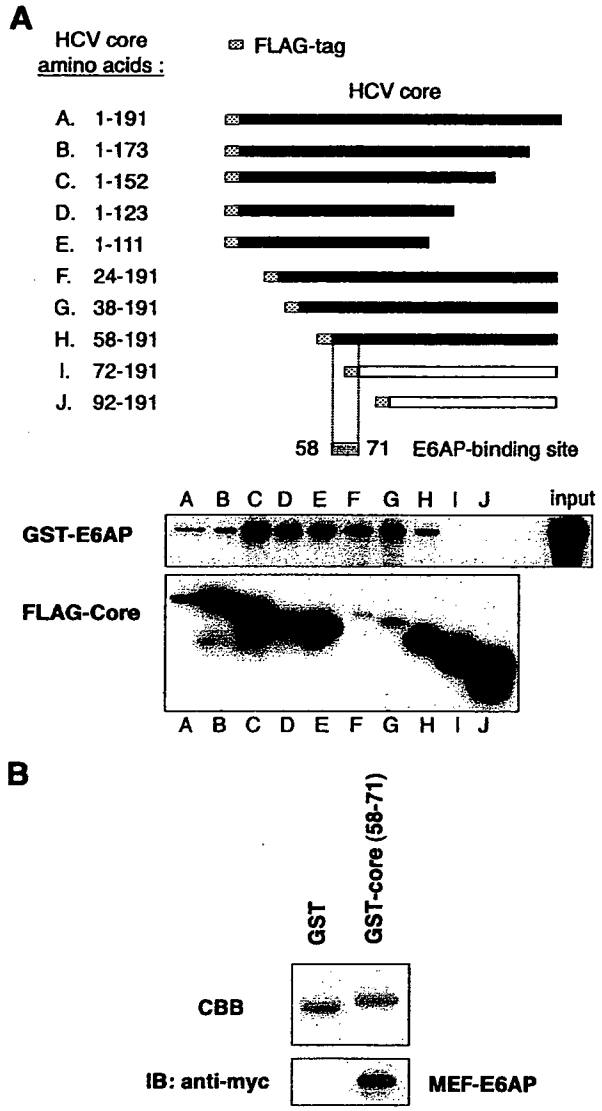

FIG. 3. Mapping of the E6AP binding domain for HCV core protein. (A) In vitro binding of E6AP to HCV core protein. 293T cells were transfected with each plasmid indicated in the upper panel. At 48 h posttransfection, cell lysates were mixed with purified GST-E6AP, immunoprecipitated with anti-FLAG beads, and then immunoblotted with anti-GST PAb (middle panel) or anti-FLAG MAb (bottom panel). The last lane (input) represents GST-E6AP used in this assay (middle panel). (B) Binding of GST-core (aa 58 to aa 71) to purified MEF-E6AP. GST served as a negative control for binding. Upper panel, Coomassie blue-stained SDS-PAGE of GST and GST-core (58–71). Lower panel, results of the GST pull-down assay. MEF-E6AP was detected by anti-myc MAb. CBB, Coomassie brilliant blue; IB, immunoblot.

duplex reduced the protein level of E6AP by 90% at 48 h posttransfection (Fig. 4C, middle panel). Immunoblotting revealed a 4.1-fold increase in the level of the core protein in the cells transfected with E6AP siRNA (Fig. 4C, top panel), suggesting that endogenous E6AP plays a role in the proteolysis of the HCV core protein.

Then we examined whether E6AP reduces the steady-state

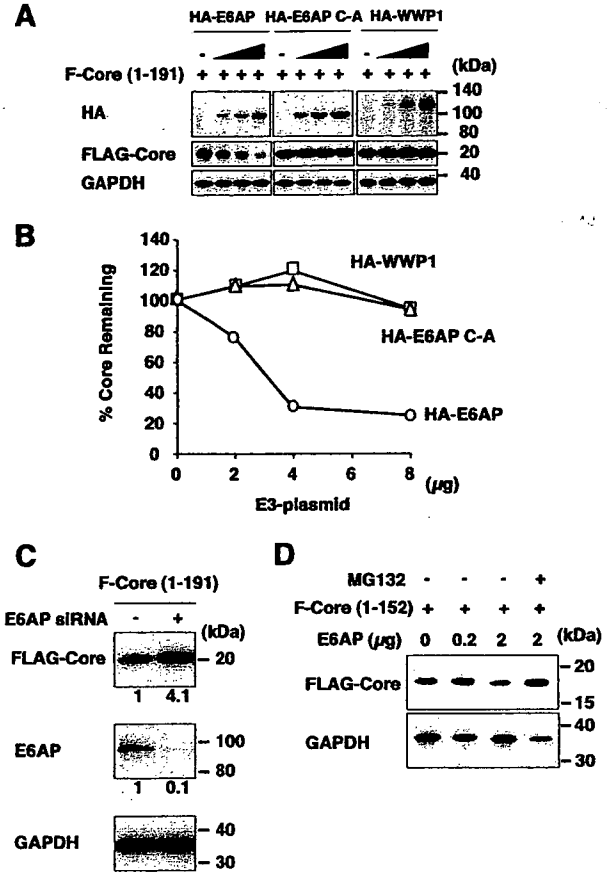

FIG. 4. E6AP decreases steady-state levels of HCV core protein in 293T cells and in HepG2 cells. (A) 293T cells (1×10^6 cells/10-cm dish) were transfected with 1 μg of pCAG FLAG-core (1–191) along with either pCAG-HA-E6AP, pCAG-HA-E6AP C-A, or pCAG-HA-WWP1 as indicated. At 48 h posttransfection, protein extracts were separated by SDS-PAGE and analyzed by immunoblotting with anti-HA PAb (top panel), anti-FLAG MAb (middle panel), and anti-GAPDH MAb (bottom panel). (B) Quantitation of data shown in panel A. Intensities of the gel bands were quantitated using the NIH Image 1.62 program. The level of GAPDH served as a loading control. Circles, E6AP; triangles, E6AP C-A; squares, WWP1. (C) Knockdown of endogenous E6AP by siRNA inhibits degradation of HCV core protein in 293T cells. 293T cells (3×10^5 cells/six-well plate) were transfected with 40 pmol of E6AP-specific duplex siRNA (or control siRNA) as described in Materials and Methods. The cells were transfected with 2 μg of FLAG-core (1–191) expression plasmid and cultured for 24 h, harvested, and analyzed by immunoblotting. Shown is immunoblot detection of FLAG-tagged core protein (top panel), E6AP protein (middle panel), and GAPDH (bottom panel) in control siRNA-treated 293T cells or E6AP-siRNA-treated 293T cells. The relative levels of protein expression were quantitated by densitometry and indicated below in the respective lanes. GAPDH served as a loading control. (D) HepG2 cells (2×10^5 cells/six-well plate) were transfected with pCAG FLAG-core (1–152) along with either empty vector or pCMV E6AP as indicated. The cells were harvested at 44 h posttransfection. Where indicated, cells were treated with 25 μM MG132 or with dimethyl sulfoxide control 14 h prior to collection. Equivalent amounts of the whole-cell lysates were separated by SDS-PAGE and analyzed by immunoblotting with anti-FLAG MAb (upper panel) or anti-GAPDH MAb (lower panel).